Max-Planck-Institut für Sonnensystemforschung

Katlenburg-Lindau, Germany

Remote sensing of plasma boundaries by finite ion gyroradius effects: applications for the RAPID instrument on Cluster.

Patrick W Daly and Urs Mall

Abstract

Finite gyroradii of energetic ions act as a probe extending to large distances beyond their detection point. For example, 30 keV protons in a field of 10 nT have a gyroradius of 2500 km. We review how this feature was exploited on the ISEE spacecraft to detect the motion of the magnetopause, passing flux transfer events, and the plasma sheet in the distant geomagnetic tail.

The IIMS ion detection system on the RAPID instrument is ideally suited to this analysis method, since it very quickly (within a 4 s spin) obtains an ion flux distribution in all directions, producing a snapshot of a distant boundary as seen from one point of measurement. With four spacecraft, the simultaneous snapshots may be superimposed to generate a larger scale view of the boundary, permitting curvature and accelerations to be determined.

The Gyromotion of a Charged Particle

The Gyroradius

A charged particle moving with velocity $\boldsymbol{v}$ through a magnetic field $\boldsymbol{B}$ describes a "gyromotion" about the field of frequency and (vector) radius

$$\omega = \frac{qB}{m} \quad ; \qquad R_g = \frac{m}{qB^2}\, \boldsymbol{v} \times \boldsymbol{B} \qquad (1)$$

For example, a 100 keV proton in a 10 nT field has a gyroradius of 4600 km, comparable to the scale lengths of magnetospheric processes. For heavier ions, the gyroradius is even larger, while for electrons, they are $\sim$ 100 km or less, i.e. almost negligible.

Gradient Anisotropy of Ion Fluxes

At a given measurement point, ion fluxes observed from different directions have gyrocenters displaced around that point (Fig. 1). The fluxes are constant on each gyro-orbit; different directions thus probe the ion densities at distances removed from the spacecraft.
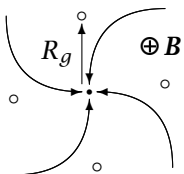

Fig. 1: Ion measurements made at the black dot reflect the densities at the open circles, the gyrocenters. From Schwartz et al. (1998).

If the ion density changes slowly over a gyroradius, the measured flux at the spacecraft exhibits an anisotropy:

$$f_{sc}(\hat{\boldsymbol{v}}) = f_0\,[1 + \hat{\boldsymbol{v}}\cdot\boldsymbol{\varepsilon} + \cdots] \qquad (2)$$

$$\boldsymbol{\varepsilon} = \frac{m v}{qB^2}\boldsymbol{B} \times \nabla \ln f_0 \qquad (3)$$

where $\hat{\boldsymbol{v}}$ is the unit vector in direction $\boldsymbol{v}$. Fitting the angular dependence of the observed f_{sc} to Eq. 2, one may determine the anisotropy $\boldsymbol{\varepsilon}$ and thus the density gradient from Eq. 3.

Remote Sensing of Boundaries

If the density gradients are very sharp, as at a boundary such as the magnetopause, Eqs. 2 and 3 no longer apply. Instead, one considers the displaced gyrocenters as distant probes around the spacecraft that encounter the boundary at different times. Hence the term *remote sensing*.
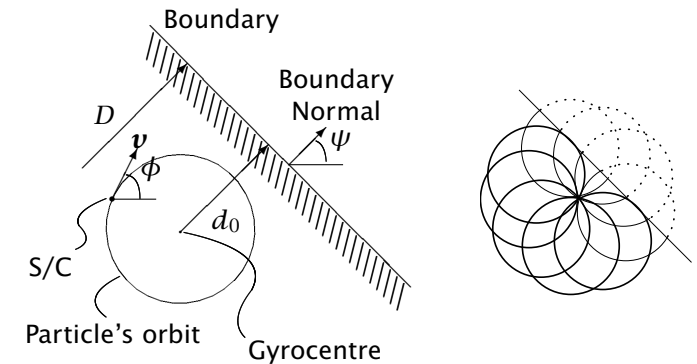

Fig. 2: Left: the gyro-orbit entirely inside an "absorbing" boundary. Right: snapshot of the boundary position, thick circles are orbits not crossing the boundary (high fluxes) while thin arcs are those that do cross, and are thus empty (low fluxes). From Schwartz et al. (1998).

At the magnetopause, where the magnetic field geometry changes radically, gyro-orbits cannot be maintained across it; an ion crossing this boundary may or may not return, and even if it does return, it will certainly be displaced from its original orbit, with a different pitch angle. This is an *absorbing boundary*, (Fig. 2).

In this case, when the s/c is within two gyroradii of the boundary, the ion distribution exhibits asymmetries at constant pitch angle but different azimuths (or phase angle). The asymmetry increases as the boundary approaches, as illustrated in Fig. 4.

Remote Sensing with ISEE S/C

The energetic particle experiments ($E > 24\,\mathrm{keV}$) on board ISEE-1 and 2 (Williams et al. 1978) have been used to remote sense magnetospheric boundaries.
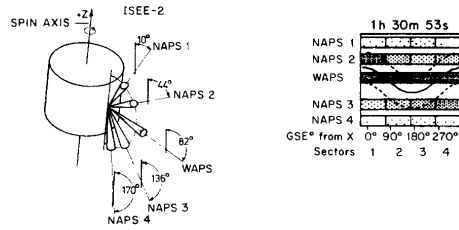
Fig. 3: The MEPE detector on ISEE-2, consisting of 5 particle telescopes mounted at fixed angles to the spin axis. Complete sampling of all directions can be achieved in a single spin. The gray-scale plot at right shows a ion intensity distribution over elevation and spin azimuth (4 sectors in this case). The solid curve is the locus of the 90° pitch angles, while the dashed curves are those for 60° and 120°. From Fritz et al. (1982).

Whereas ISEE-1 possesses a single particle telescope on a moving platform, sampling all elevation angles in 12 spins, ISEE-2 with its 5 telescopes (Fig. 3) samples in all directions within 1 spin (3 s). There can be as many as 32 spin sectors, depending on bit-rate. In practice, the large time resolution on ISEE-1 makes remote sensing studies difficult.

The Magnetopause

Fritz et al. (1982) used this technique to sense the ion trapping boundary and to establish that it is associated with the magnetopause as determined by magnetic field measurements. Fig. 4 shows how the ion asymmetry waxes and wanes as the magnetopause approaches and recedes.
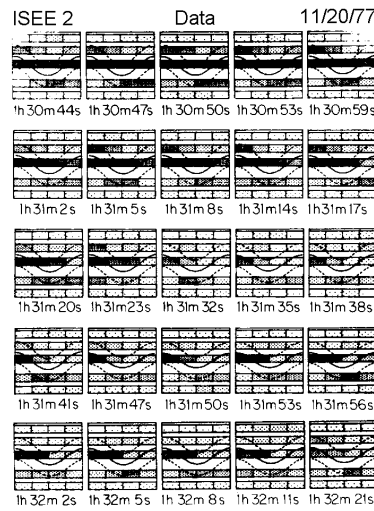
Fig. 4: Remote sensing of the magnetopause with ISEE-2 by Fritz et al. (1982). The azimuthal asymmetries at a given pitch angle increase as the magnetopause approaches. Initially the fluxes at 90° are symmetric (top panel) becoming more pronounced in panels 2–4. In the 5th panel, the asymmetry reduces as the boundary retreats.

Sensing Flux Transfer Events

Daly & Keppler (1983) have sounded the passage of an FTE over the ISEE-2 s/c to determine its size (1–$2\,R_E$) and speed (50–$100\,\mathrm{km/s}$ in the magnetopause plane). Snapshots of its passage are shown in Fig. 5.

Fig. 5: The passage of an FTE over the ISEE-2 s/c as determined by a best fit of the times when ions at different azimuths suddenly exhibited high fluxes (solid circles). Dashed circles are ion orbits of low flux. From Daly & Keppler (1983).
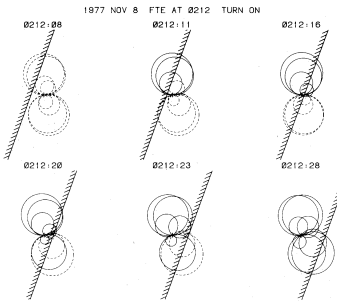
The Plasmasheet in the Geotail

A similar experiment on ISEE-3 consists of three particle telescopes at fixed elevation angles. During its exploration of the Earth's magnetotail, it was able to remotely probe the plasmasheet. Here the field is either earthward or anti-earthward so that the dawnward and duskward fluxes correspond to gyrocenters to the north and south of the s/c. Flux measurements are shown in Fig. 6 and resulting contour line density maps of the plasmasheet in Fig. 7.
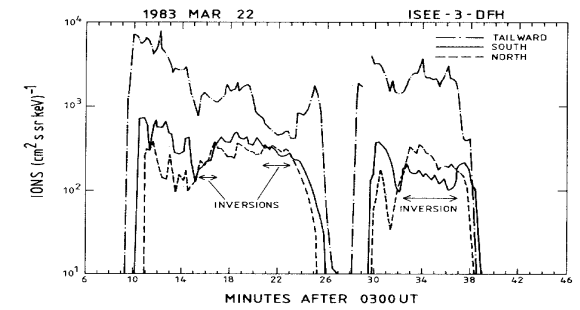
Fig. 6: Ion fluxes at 3 azimuths of one ISEE-3 ion telescope. The labels *north* and *south* refer to the gyrocenters of the ion orbits of the two 90° pitch angle azimuths; *tailward* is the flux along the magnetic field, away from the Earth.
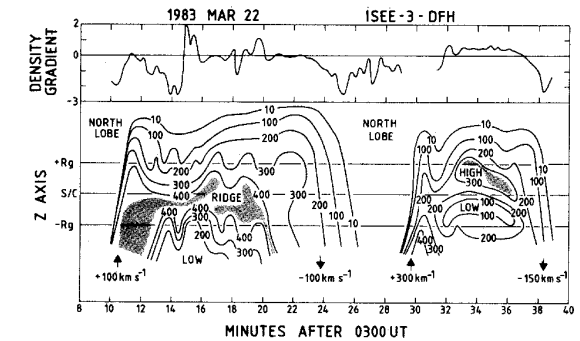
Fig. 7: A density map of the plasmasheet reconstructed from the data in Fig. 6. Both from Daly et al. (1984).

Applications for RAPID

Remote sensing of particle boundaries is a proven technique from the ISEE experiments, provided adequate sampling of sufficient directions can be carried out fast enough, i.e. within a few seconds.

The prospects for the RAPID experiment on Cluster (Wilken et al. 1997) are therefore very good. It measures ion fluxes in 12 elevation angles, sorted into 16 azimuthal sectors. Of these, those fluxes at 90° to the magnetic field will be of most interest for probing the various magnetospheric boundaries that Cluster is likely to encounter. Snapshots of the boundary such as those of Fig. 5 will be available from 4 spacecraft, providing a very graphic representation of the boundary shapes, distances, and motion.

Ion Spectrometer   Electron Spectrometer
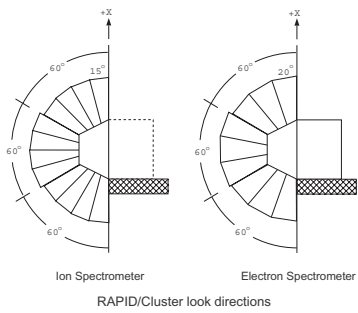
RAPID/Cluster look directions

Fig. 8: The RAPID ion spectrometer (left) observes at 12 elevation angles while the electron spectrometer (right) at 9. Spin sectorization produces 16 azimuthal bins.

Fig. 9: The RAPID experiment with the ion (left) and electron (right) spectrometers.

References

Daly P.W., Keppler E., 1983, J. Geophys. Res., 88, 3971

Daly P.W., Wenzel K.P., Sanderson T.R., 1984, Geophys. Res. Lett., 11, 1070

Fritz T.A., Williams D.J., Paschmann G., Russell C.T., Speldvik W.N., 1982, J. Geophys. Res., 87, 2133

Schwartz S.J., Daly P.W., Fazakerley A.N., 1998, In: Paschmann G., Daly P.W. (eds.) Analysis Methods for Multi-Spacecraft Data, no. SR-001 in ISSI Scientific Reports, chap. 7, 159–183, ESA Publ. Div., Noordwijk, Netherlands

Wilken B., Axford W.I., Daglis I., et al., 1997, Space Sci. Rev., 79, 399, URL http://www.wkap.nl/oasis.htm/124389

Williams D.J., Fritz T.A., Wilken B., Keppler E., 1978, IEEE Trans. Geosci. Electron., GE-16(3), 270